

OPEN

Production of adeno-associated virus vectors for *in vitro* and *in vivo* applications

Toyokazu Kimura^{1,3}, Beatriz Ferran¹, Yuko Tsukahara¹, Qifan Shang¹, Suveer Desai¹, Alessandra Fedoce¹, David Richard Pimentel², Ivan Luptak², Takeshi Adachi³, Yasuo Ido³, Reiko Matsui¹  & Markus Michael Bachschmid¹ 

Delivering and expressing a gene of interest in cells or living animals has become a pivotal technique in biomedical research and gene therapy. Among viral delivery systems, adeno-associated viruses (AAVs) are relatively safe and demonstrate high gene transfer efficiency, low immunogenicity, stable long-term expression, and selective tissue tropism. Combined with modern gene technologies, such as cell-specific promoters, the Cre/lox system, and genome editing, AAVs represent a practical, rapid, and economical alternative to conditional knockout and transgenic mouse models. However, major obstacles remain for widespread AAV utilization, such as impractical purification strategies and low viral quantities. Here, we report an improved protocol to produce serotype-independent purified AAVs economically. Using a helper-free AAV system, we purified AAVs from HEK293T cell lysates and medium by polyethylene glycol precipitation with subsequent aqueous two-phase partitioning. Furthermore, we then implemented an iodixanol gradient purification, which resulted in preparations with purities adequate for *in vivo* use. Of note, we achieved titers of 10^{10} – 10^{11} viral genome copies per μl with a typical production volume of up to 1 ml while requiring five times less than the usual number of HEK293T cells used in standard protocols. For proof of concept, we verified *in vivo* transduction via Western blot, qPCR, luminescence, and immunohistochemistry. AAVs coding for glutaredoxin-1 (Glrx) shRNA successfully inhibited Glrx expression by ~66% in the liver and skeletal muscle. Our study provides an improved protocol for a more economical and efficient purified AAV preparation.

Delivering a gene of interest to cells or animals has become an essential technique in biomedical research. In recent years, adeno-associated viruses (AAVs) have been used for many *in vitro* and *in vivo* applications due to their high transduction efficiency, safety, and extended stable gene expression. Furthermore, several recent clinical trials demonstrated the full potential of AAVs for human gene therapy^{1–4}.

AAVs belong to the *Parvoviridae* family and are small non-enveloped viruses containing a linear single-stranded (ss) DNA⁵. Wild-type AAVs, as part of their lysogenic cycle, can integrate into the AAVS1 site of human chromosome 19 or rarely at random locations⁶. AAVs engineered for research or gene therapy, however, do not incorporate into the genome and instead form episomal concatemers in the host cell nucleus⁷. These head-to-tail circular concatemers remain intact in non-dividing cells but are lost during mitosis. Thus post-mitotic tissues, such as neurons and cardiomyocytes, may express transgenes over several months⁸.

AAVs are ideal for gene therapy due to their low immunogenicity, restricted generation of neutralizing antibodies, and replication defectiveness. AAV production requires cytopathogenic effects, which only occur after co-infection with a helper adenovirus or herpesvirus^{8,9}. Helper viruses are difficult to remove and may induce undesired effects such as inflammation in the host. Current AAV expression systems avoid using helper viruses and include the plasmid pHelper instead⁸, containing essential genes such as E2A and E4. Human embryonic kidney cells (HEK) 293T cells, which express SV40 large T antigen, supply additional necessary proteins⁹. This AAV production system is referred to as ‘helper-free’ and consists of three different plasmids encoding essential

¹Vascular Biology Section, Whitaker Cardiovascular Institute, Boston University School of Medicine, Boston, USA.

²Cardiology, Whitaker Cardiovascular Institute, Boston University School of Medicine, Boston, USA. ³Cardiovascular Medicine, National Defense Medical College, Tokorozawa, Japan. Toyokazu Kimura, Beatriz Ferran, Reiko Matsui and Markus Michael Bachschmid contributed equally. Correspondence and requests for materials should be addressed to R.M. (email: rmatsui@bu.edu) or M.M.B. (email: bach@bu.edu)

Received: 18 September 2018

Accepted: 11 July 2019

Published online: 19 September 2019

viral and helper genes: pHelper, AAV trans-plasmid comprising AAV replication (*Rep*) and capsid (*Cap*) genes, and AAV cis-plasmid encoding the gene of interest, promoter, and inverse terminal repeats (ITRs)¹.

Early work used the capsid and viral machinery derived from AAV serotype 2 (AAV2). AAV2 is still the basis for most AAV systems, but now, engineered capsids including DJ and DJ8 with tissue-specific tropisms or higher infectivity are available¹⁰. The DJ serotype also shows efficient transfection of many cultured cells, making DJ especially suitable for cell culture and *in vivo* applications. Furthermore, specific promoters, the Cre/flox system, and gene editing via CRISPR render AAVs cell-specific and allow novel approaches in gene therapy and animal research. Most protocols recommend AAV purification from lysates of producer cells, grown in large cell stacks or cell culture factories to obtain sufficient AAVs for animal experiments¹¹. However, producer cells also release large quantities of AAV into the culture medium^{12–16}, which often remains unused. Combining reported techniques, we optimized our protocol to obtain AAVs and purify the viral particles from producer cells and medium efficiently.

We tested several published protocols, most of which are labor-intensive, have low virus yields, and often result in contaminated virus preparations. We developed a revised protocol that is economical and efficient for the majority of laboratories with conventional equipment and reagents. For proof of concept, we evaluated the *in vivo* and *in vitro* efficacy of the viral particles by AAV-mediated short hairpin glutaredoxin-1 (*Glrx*) gene knockdown.

Materials and Methods

Reagents, materials and antibodies. HEK293T (ATCC[®] CRL3216[™]) human embryonic kidney and the mouse myoblast cell line C2C12 (ATCC[®] CRL1772[™]) were obtained from ATCC (Manassas, VA). Dulbecco's modified Eagle medium (DMEM) and the penicillin/streptomycin cocktail were obtained from Gibco (Grand Island, NY) and the fetal bovine serum (FBS) was obtained from Atlanta Biologicals (Flowery Branch, GA). pAAV-DJ Rep-Cap plasmid (VPK-420-DJ), and pAAV-DJ/8 Rep-Cap plasmid (VPK-420-DJ-8) were purchased from Cell Biolabs (San Diego, CA). pHelper (Accession #: AF369965), pAAV-R2C6 (Accession #: AF369963), and pAAV-MCS (Accession #: AF396260) were obtained from Stratagene (CA, USA). The pCR8 vector was part of the Invitrogen TOPO cloning kit (K250020), and the Gateway system containing LR Clonase was from Invitrogen (Thermo Fisher Scientific, Waltham, MA).

Anion exchange columns and miniprep silica columns were from Epoch Life Science (Sugar Land, TX), silver nitrate solution and polyethyleneimine (PEI) were from Polysciences (Warrington, PA). Pluronic P68 and Optiprep[™] Axis-Shield (Dundee, Scotland) were ordered from Sigma-Aldrich (St. Louis, MO). Amicon Ultra-15 Centrifugal Filter Units (100,000 MWCO) were from Millipore (Burlington, MA). Type 70.1 Beckman rotor and Quick-Seal Centrifuge Tubes (Polypropylene, 13.5 ml, 16 × 76 mm) were obtained from Beckman Coulter (Brea, CA). Anti-green fluorescent protein (GFP) rabbit polyclonal antibody (PA1-980A), which also recognizes mVenus was obtained from Thermo Fisher Scientific (Waltham, MA). Anti-Glrx goat antibody (AGRX-03) was from IMCO (Solna, Stockholm). Polyvinylidene fluoride (PVDF) membrane for Western blot was obtained from GE Healthcare (Little Chalfont, Buckinghamshire). Precision Plus[™] Protein Prestained Protein Standards (10–250 kD) and acrylamide 37.5:1 solution were obtained from Bio-Rad (Hercules, CA). Western blots were developed using Kwik Quant peroxidase substrate and imager (Kindle Biosciences, Boston, MA). NEB Stable competent *E. coli* and BioLux Gaussia Luciferase Assay Kit were purchased from New England BioLabs (Ipswich, MA). All other supplies were bought from Thermo Fisher Scientific (Waltham, MA).

Animals. Male C57BL/6J mice were obtained from The Jackson Laboratory (Sacramento, CA). Mice were maintained in the animal facility at Boston University Medical Campus on a 12-hour light-dark cycle and fed standard chow *ad libitum*. C57BL/6J mice were retro-orbitally injected with 100 µl of a viral preparation containing 5×10^{11} virus genomes (vg) encoding short hairpin Glrx (AAV2-DJ/8-shGlrx-mVenus) or hairpin Control (AAV2-DJ/8-shControl-mVenus) in saline (titers were measured with ITR primers). Different amounts of AAV expressing secreted Gaussia luciferase (AAV2-DJ/8-Gluc; 1.5×10^{11} vg/µl; injection volume 25 µl, 50 µl, and 100 µl; titer was measured with ITR primers) were administered via the tail vein. To locally transduce the skeletal muscle, 50 µl containing 4.4×10^{12} vg of AAV2-6-shGlrx-mVenus or AAV2-6-shControl-mVenus was administered via intramuscular (IM) injection (titers were measured with ITR primers). Mice were euthanized 2 to 6 weeks after virus administration. The protocol AN-15526 was approved by the Institutional Animal Care and Use Committee at Boston University School of Medicine.

AAV cloning. The “Helper-free” AAV system comprised of pHelper, pAAV-MCS, pAAV-R2C6, was purchased from Stratagene (San Diego, CA) and capsid encoding plasmids pAAV-DJ and pAAV-DJ/8 were from Cell Biolabs (San Diego, CA). See ‘reagents, materials, and antibodies’ section and supplement for order details, accession number, plasmid maps, and sequence information. mVenus was inserted at the HindIII site of pAAV-MCS. A Gateway cassette (attB1 and attB2) was inserted at MluI site to facilitate the insertion of the U6 promoter expression cassette. Control shRNA (target sequence: ACACCTATACAACGGTA) and mouse Glrx short hairpin RNA (shRNA; target sequence: AGTCCACTTCTAAAGAA) were cloned as described previously¹⁷, and a CMV enhancer sequence was added upstream of the U6 promoter to enhance shRNA expression¹⁸. The shRNA expression cassette was designed according to the guidelines published by Miyagishi *et al.*¹⁹ introducing a 17 nucleotide (nt) counting double strand stem with a 21 nt long loop (GCTGCGTTCAAGAGATGCGGT). The shRNA construct was created by tandem PCR with human U6 promoter. These sequences were inserted in the pCR8 vector, and the AAV plasmid expressing shRNA and mVenus was created by LR reaction according to the manufacturer's instructions (please find sequence maps in the supplement). AAVs were produced by co-transfection of pHelper, pAAV ITR-expression vector, and pAAV *Rep-Cap* genes in a 1:1:1 molar ratio normalized to the plasmid size (see supplement).

Plasmids were prepared by alkaline lysis followed by anion-exchange chromatography (Epoch Life Science, Sugar Land, TX) and isopropanol glass filter-assisted precipitation. A low-cost plasmid preparation protocol is provided as Supplementary Information. The integrity of isolated plasmids was verified by restriction enzyme digestion with PvuII, ApaLI and ApaI and agarose gel electrophoresis. The identity of all constructs was confirmed by sequencing using the Genewiz (Boston, MA) services.

AAV production and purification. The detailed protocol for AAV purification is provided as Supplementary Information. Briefly, 50–70% confluent HEK293T cells grown in DMEM supplemented with 5% FBS were triple transfected with pHelper, pAAV ITR-expression, and pAAV Rep-Cap plasmids using acidified PEI²⁰ in five T150 flasks. After transfection, two medium changes to DMEM with FBS were performed. At day 5 post-transfection, media and cells were collected and processed separately. Cells were lysed in an acidic buffer, the homogenates were cleared from debris by centrifugation, and the pH was neutralized using HEPES buffer. AAVs were precipitated from lysates and medium with polyethylene glycol (PEG) 8000. The PEG-precipitated AAV was collected by centrifugation, followed by chloroform and an aqueous two-phase extraction in ammonium sulfate and PEG 8000^{21,22}. For *in vivo* use, AAVs were further purified using discontinuous iodixanol gradient ultracentrifugation^{23,24}. Three different pAAV Rep-Cap plasmids were used: pAAV-DJ (VPK-420-DJ, Cell Biolabs), to obtain AAV2-DJ particles for the *in vitro* studies; pAAV-DJ/8 (VPK-420-DJ-8, Cell Biolabs), to address the *in vivo* transduction to the liver by AAV2-DJ/8 particles; and pAAV-R2C6 (pAAV-RC AF369963, Stratagene), to obtain virions with AAV2-6 serotype and address the transduction to the skeletal muscle.

AAV titration and purity assessment. Primers binding within the AAV2 ITRs²⁵ were used to measure the virus titer with quantitative polymerase chain reaction (qPCR). Before releasing the viral DNA from the particles, all extra-viral DNA was removed by digestion with DNase I. Then, the viral DNA was released by alkaline lysis. The qPCR was performed using the PowerUp™ SYBR™ Green Master Mix (Applied Biosystems, Foster City, CA), and primers against the ITRs and a primer pair that amplifies the short hairpin cassette (Forward: GTGGAAAGGACGAAACACCG; Reverse: GCTCCAAGGATCATCAACCAC) obtained from Invitrogen (Carlsbad, CA). The extracted viral DNA and a serial dilution of a viral plasmid containing ITRs and the short hairpin cassette as a standard were measured using the CFX96 Touch Real-Time PCR Detection System and the CFX Maestro Software (Bio-Rad, Hercules, CA). For details about AAV extraction and analysis, please refer to the Supplementary Information.

AAV capsid proteins were separated by sodium dodecyl sulfate-polyacrylamide gel electrophoresis (SDS-PAGE) and detected with fast silver staining to assess the purity of viral preparations^{26–28}. Serial dilutions of bovine serum albumin (BSA; Sigma-Aldrich, St. Louis, MO) were used as protein standards. Images were obtained using an Epson scanner (Epson Perfection V800 Photo, Digital ICE Technologies). A detailed protocol is provided as Supplementary Information.

Cell culture. Experiments were performed on primary hepatocytes from C57BL/6J mice and the C2C12 cell line. Cells were cultured in 12-well plates in high glucose DMEM containing 10% FBS and penicillin/streptomycin. C2C12 cells were made quiescent by reducing FBS to 1% in the medium. Cells were transduced with AAV containing either short hairpin Glrx (AAV2-DJ-shGlrX-mVenus) or short hairpin Control (AAV2-DJ-shControl-mVenus) at 1.56×10^6 vg per well (titers were measured with ITR primers). Six days after infection, cells were harvested for further analysis of RNA and protein levels. Glucose concentrations were measured using a Contour Next One blood glucose meter and a single use glucose test strip (Bayer, Ascensia Diabetes Care, Parsippany, NJ) with 1 μ l of cell culture medium. Acidification was measured with a Mettler Toledo (Columbus, OH) LE422 micro pH electrode.

Luciferase activity assay. Four groups of four male mice were injected with either phosphate buffered saline (PBS) or AAV to overexpress the *Gaussia* Luciferase, as previously described in the “Animals” section. Blood was collected from the tail vein at 1–3 week intervals after AAV injection. Serum was separated from red cells by centrifugation at $1,000 \times g$ at 4 °C for 10 minutes. Luciferase activity was measured in the serum with a BioLux *Gaussia* Luciferase Assay Kit according to the manufacturer’s protocol using a TD-20e Luminometer (Turner BioSystems, Sunnyvale, CA).

Western blotting. Tissues or cell monolayers were homogenized in lysis buffer composed of 50 mM Tris pH 7.4, 150 mM NaCl, 5 mM EDTA, 1% NP-40, and supplemented with cComplete™ Mini Protease Inhibitor Cocktail (Roche Applied Science, Penzberg, Germany). After removing the debris by centrifugation, the protein concentration of lysates was measured with the DC™ Protein Assay (Bio-Rad, Hercules, CA). Protein samples were prepared under reducing conditions, and 50 μ g of total protein per lane were loaded on a NuPAGE 4–12% Bis-Tris gel (Invitrogen, Carlsbad, CA). After transferring proteins to a PVDF membrane using a Trans-Blot™ Turbo Transfer System (Bio-Rad, Hercules, CA) and blocking with 5% non-fat dry milk powder (NFDm), the blots were incubated overnight at 4 °C with anti-GFP, anti-GlrX, and anti- β -tubulin antibodies, all diluted 2000-fold in 5% BSA. After incubating the blots for 1 hour with corresponding HRP-conjugated antibodies (diluted 5000-fold in 5% NFDm), the chemiluminescent signal was detected using the Hi/Lo Digital-ECL™ Western Blot Detection Kit and the KwikQuant™ Imager. The bands of interest were quantified using the ImageJ software.

Reverse transcription (RT) and the quantitative polymerase chain reaction. Total RNA was extracted from cells or tissues with TRIzol reagent (Invitrogen, Carlsbad, CA) and the Direct-zol RNA MiniPrep Plus kit (Zymo Research, Irvine, CA). cDNAs were synthesized from 1 μ g of total RNA using the High-Capacity RNA-to-cDNA™ kit (Applied Biosystems, Foster City, CA) according to the manufacturer’s instructions. Quantitative PCR was performed using TaqMan primers (Applied Biosystems, Foster City, CA)

Glr_x (Mm00728386_s1) and Actb (Mm01205647_g1) using CFX96 Touch Real-Time PCR Detection System and CFX Maestro Software (Bio-Rad, Hercules, CA). Expression changes were calculated by the comparative Ct ($\Delta\Delta C_t$) method.

Immunofluorescence. Liver sections (10 μ m) were cut with a Leica CM1950 Clinical Cryostat (Leica, Wetzlar, Germany), washed with PBS three times (3–5 minutes each time), fixed with 4% paraformaldehyde (PFA) in PBS for 10 minutes, and rinsed in PBS three times at room temperature. Samples were then blocked in 5% NFD in PBST for 1 hour at room temperature. Rabbit anti-GFP (1:200, PA1-980A; ThermoScientific Pierce Products) was used as primary antibody in 5% NFD in PBST and samples were incubated overnight at 4 °C. Sections were washed three times in PBS and incubated with the secondary antibody Alexa Fluor 594 (1:200, R37117; Thermo Scientific Pierce Products) and Hoechst 33342 (1:2000, H3570; Bioprobes) for 1 hour at room temperature. After incubation, slides were washed three times and mounted using FluorSave Reagent (Calbiochem). Individual images were acquired using the HS All-in-one Fluorescence Microscope BZ-9000E (Keyence, Osaka, Japan) with a 20x objective and the BZ-II Analyzer (Keyence, Osaka, Japan).

Statistical analysis. Statistical analysis was performed using Prism 5.0 (GraphPad Software, La Jolla, CA). Means were compared between two groups by student's t-test and two-tailed Mann-Whitney tests. More than two groups were analyzed with the non-parametric Kruskal-Wallis test followed by Dunn's multiple comparison post-test. P values < 0.05 were considered statistically significant. The error was reported as the standard error of the mean (SEM).

Regulatory. All experimental protocols were approved by Boston University Institutional Animal Care & Use Committee (IACUC) under animal protocol AN-15526 and Boston University Institutional Biosafety Committee (IBC) under protocol 16-983. All methods were carried out in accordance with the relevant and approved guidelines and regulations.

Results

Serotype-independent purification of AAVs. Depending on the AAV serotype, HEK293T cells release a significant amount of the virus into the medium without cytopathic effects^{12–15}. AAV2- and DJ-capsid based viruses, however, may remain bound to the cell surface via an intact heparin binding domain¹². Reports have shown that serum reduction and mildly alkaline pH increase AAV production²⁹. We tested several culture conditions to determine whether cells in an optimal or stress environment can promote viral production. Standard Dulbecco Modified Eagle Medium (DMEM) to grow HEK293T cells contains 25 mM of glucose and glutamine as a carbon and energy source as well as fetal bovine serum to sustain cell growth. Since glutamine spontaneously decomposes to form ammonia during storage and long-term culture, we employed the alternative GlutaMAX (L-alanyl-L-glutamine dipeptide). GlutaMAX can minimize ammonia build-up and media exhaustion during culture³⁰. Due to protein contamination from fetal bovine serum after iodixanol purification (mainly albumin; protein band at 66 kDa), we initially reduced the fetal bovine serum to 1%. The reduced serum quantities minimally impacted the viral titer on either day 3 or 5 (Fig. 1A–C).

Upon viral protein expression, marked media acidification occurred on day 3 and 5 in standard 25 mM glucose (4.6 g/l) containing DMEM. The initial pH dropped from 8.0 to below 7.0 (Fig. 1A). To increase the buffering capacity of the 25 mM glucose DMEM and delay acidification, we supplemented the medium with cell culture compatible amounts of sodium bicarbonate and HEPES. Even in the presence of high amounts of the buffering compounds, the pH still dropped below 7.0 on day 3 and 5 with only a mild increase in viral quantity (Fig. 1C). As the releases of lactate from glycolysis is a common cause of cell culture medium acidification, we speculated that limiting glucose may prevent media acidification and increase viral particles. For further determination of the effect of glucose, we cultured AAV-producing cells in 5 mM glucose (1 g/l) DMEM with the same amounts of sodium bicarbonate and HEPES buffering, FBS, and stable glutamine. The pH stabilized at ~7.4 and glucose concentration dropped below the detection limit but the viral production increased ~3-fold. These data suggest that limiting glycolysis to stabilize the pH appears beneficial for viral production. Presumably, limiting glycolysis forced cultured producer cells to derive energy and biosynthetic building blocks through glutaminolysis³¹, a well-established effect observed in cultured cells^{32,33}, immune cells³⁴, and pluripotent stem cells³⁵.

Overall, HEK293T cells showed robust AAV production under varying conditions, but in our hands, low glucose DMEM medium supplemented with 1% FBS, 1x Glutamax, 10 mM HEPES and addition of 0.075% sodium bicarbonate delivered the best results. Using this production medium and following the timeline described in the protocol, we quantified AAV2-DJ and AAV2-DJ/8 particles released at 2, 3, 4, 5 and 6 days after transfection (Fig. 1D). Producer cells released considerable amounts of viral particles at day 3, and after changing the medium, the titer increased again until day 5 to a steady level.

We tested several published protocols to purify AAVs. Most protocols are labor intensive, have low virus yields, and often result in contaminated virus preparations. Thus, we have developed a revised protocol as outlined in Fig. 2. AAVs can be concentrated and purified from cell culture medium by cost-effective PEG precipitation. The procedure includes two time points for medium collection on day 3 and 5 to increase virus yields. The delayed medium collection has negligible effects on AAV activity, which was also reported by others^{12,14,15}.

HEK293T cells contain AAVs, and most protocols use harsh lysis conditions resulting in increased contamination with cellular proteins and DNA. These lysates require further extensive processing with DNase I/ BenzonaseTM^{36,37}. In contrast, lysis of HEK293T producer cells in an acidic citrate buffer promotes AAV release with less contamination³⁸. Furthermore, citrate complexes bivalent ions and the low pH may activate an intrinsic protease activity of viral capsid proteins³⁹, likely aiding with the release of AAVs. We noted that these cell lysates prepared in acidic citrate buffer (110 mM citrate, pH 4.2) were markedly cleaner than conventional cell lysis, and

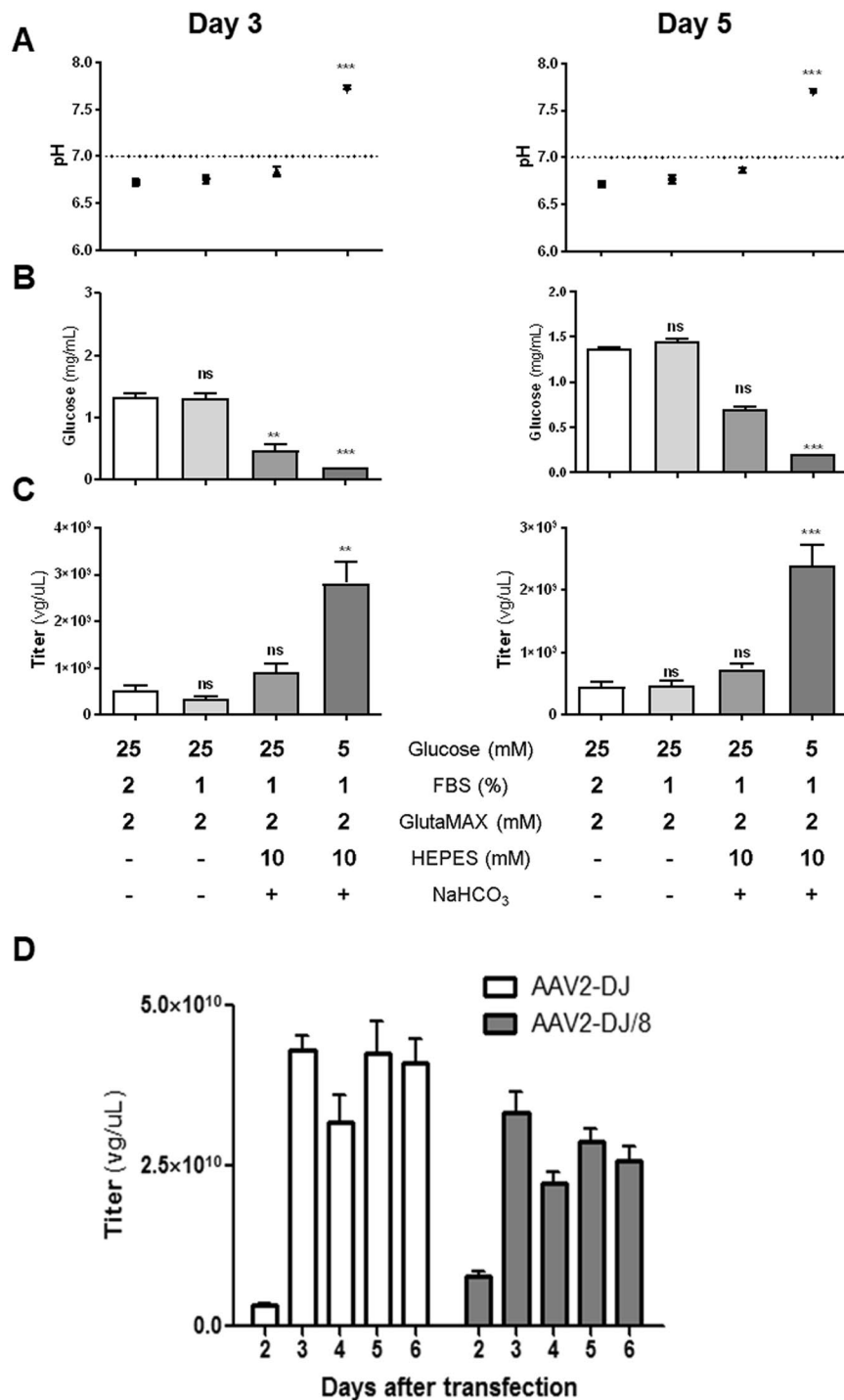


Figure 1. Comparison of AAV production using different media formulations and time points. The graph represents (A) pH, (B) glucose concentration, and (C) viral titers of AAV2-DJ-shGlr-mVenus in the cell culture medium of HEK293T cells at days 3 and 5 post-transfection with viral plasmids. HEK293T cells were cultured for AAV production in supplemented DMEM as described in the table below. Statistical analysis was performed using the non-parametric Kruskal-Wallis test followed by Dunn's multiple comparisons test. Statistical differences ($n = 8$; ns = not significant; $**P < 0.01$; $***P < 0.001$; SEM) are compared with medium containing 2% FBS as a control. (D) The graph shows titers of the released AAV2-DJ-shGlr-mVenus and AAV2-DJ/8-shGlr-mVenus into the cell culture medium at different days post-transfection. The medium was composed of DMEM, 1% FBS, 1x Glutamax, 10 mM HEPES and addition of 0.075% sodium bicarbonate. On day 3, the medium was changed ($n = 8$; SEM).

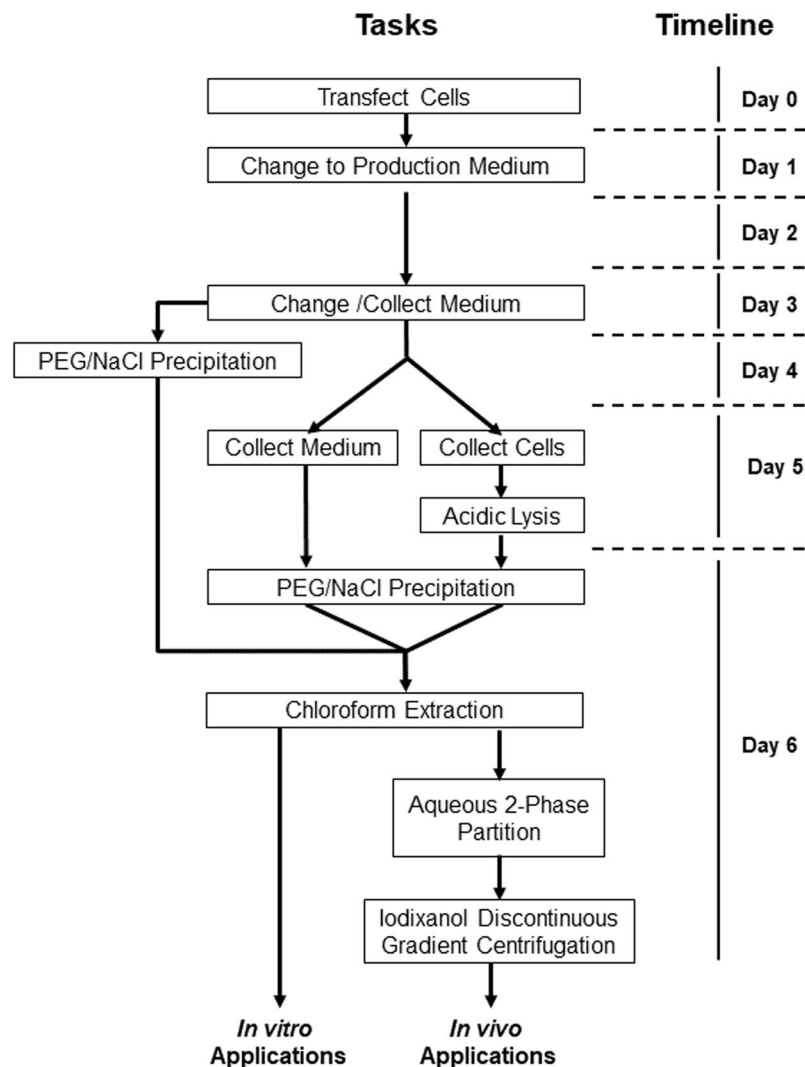


Figure 2. Flowchart of AAV purification. The helper-free AAV system comprises three types of plasmids (ITR-containing plasmid, AAV Rep-Cap plasmid, pHelper). Triple plasmid co-transfection with PEI into HEK293T cells was performed in five T150 flasks (day 0). On day 3 and day 5, 150 ml of medium were collected and subjected to AAV purification. On day 5, cells were detached with 0.5 M EDTA (pH 8.0), collected, and subjected to lysis in citrate buffer for further purification. AAVs were isolated from both cell lysate and medium, and the purification took 2 days, from day 5 to day 6. Cell lysate and medium were purified in the same manner after the PEG/NaCl precipitation. After aqueous two-phase partitioning, an iodixanol discontinuous gradient purification step was performed.

subsequent purification steps removed any residual contaminants. Prior methods have focused on mainly using cell lysates to collect viruses. We confirmed that production medium contained significant amounts of AAVs in the range of 10^8 to 10^{10} viral genomes per microliter (vg/ μ l), which allowed us to obtain final titers of 10^{10} to 10^{11} vg/ μ l of purified AAVs measured with qPCR using specific primers for the short hairpin region. However, using primers that amplify the ITR sequence, we obtained titers up to 10 times higher (in the range of 10^{11} – 10^{12} vg/ μ l). Therefore, the ITR sequence is universal but may overestimate the virus titer. Additional pilot experiments should always be performed to confirm the biological activity of the AAV^{40–43}.

Using the AAV-containing media, we performed PEG precipitation, followed by lipid extraction with chloroform and aqueous two-phase partitioning with 10% (w/w) PEG and 13.2% (w/w) ammonium sulfate²¹. This sequence of purification steps allowed for most protein contaminants to precipitate or partition into the inter- and top PEG phases. AAVs remained soluble in the ammonium sulfate phase.

For *in vivo* use, we removed the remaining contaminants with a discontinuous iodixanol (OptiPrep™) gradient ultracentrifugation^{23,24} using four layers of different iodixanol concentrations of 15, 25, 40, and 54% (Fig. 3A,B). The iodixanol gradient is also a useful step to remove empty or incomplete viral particles^{14,44–46}. The isotonic and relatively inert nature of iodixanol maintains the AAVs potency. As high amounts of iodixanol may also cause kidney toxicity in already health-compromised animals^{47–49}, we reduced the iodixanol concentration of the final virus suspension using centrifugal filter units.

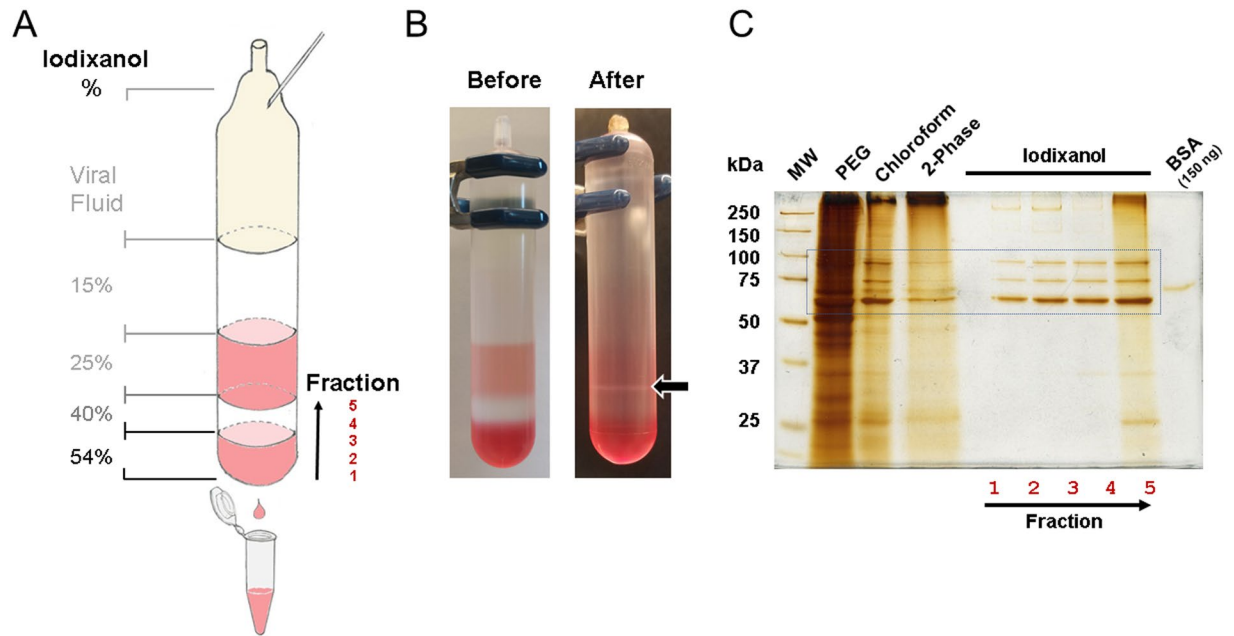


Figure 3. AAV iodixanol discontinuous gradient purification and purity assessment. **(A)** Serotype-independent purification of AAVs using a discontinuous iodixanol gradient and ultracentrifugation. The 15% iodixanol layer was underlayered with denser iodixanol solutions to create the step gradient. The 25% and 54% iodixanol layers included phenol red for better visualization. Complete AAVs concentrated in the 40% layer. For elution of the iodixanol gradient, a small hole was drilled into the bottom of the centrifuge tube using a 25 G needle and another 25 G needle was inserted at the top. Fractions of 1 ml for the 54% layer, three of 400 μ l for the 40% layer, and 1 ml for the 25% interface were collected. **(B)** Actual iodixanol step gradient before and after centrifugation. Visible interphase (arrow) between the 40% and 25% layers consists of empty and incomplete AAV2-DJ/8 particles, which may contain fragments of viral ssDNA. **(C)** Silver-stained protein gel of AAV2-DJ/8 samples at different stages of purification. Box denotes the area of the viral capsid proteins VP1 (87 kDa), VP2 (73 kDa), and VP3 (62 kDa). The purification procedure, using PEG precipitation, chloroform extraction, and aqueous two-phase extraction gradually separated contaminating proteins. The final discontinuous iodixanol gradient ultracentrifugation yielded highly purified AAV particles in fractions 2–4. The viral genome copy number measured with qPCR was high in fractions 2–4 while fraction 5 contained \sim 10 times lower copy numbers, likely due to viral particles containing ssDNA fragments carried over from the 40% layer.

To assess the purity of AAV preparations, we performed silver staining (Fig. 3C). The chloroform extraction step (lane 3) resulted in sufficiently pure AAV preparation suited for cell culture use. Fractions 2–4 collected from the 40% layer (lanes 6–8) showed three major bands corresponding to the AAV capsid proteins—virion proteins 1 (VP1; 87 kDa), 2 (VP2; 73 kDa), and 3 (VP3; 62 kDa)—with a purity greater than 90% and suitable for *in vivo* use. Samples above fraction 4 showed a band at \sim 66 kDa similar to the BSA standard, which likely represents medium-derived albumin and several other protein contaminants. Thus, iodixanol discontinuous gradient ultracentrifugation effectively removes most contaminants and results in highly purified and enriched fractions of active AAV.

Testing AAVs *in vitro*. We produced AAV2-DJ and AAV2-DJ/8 with a bicistronic expression system coding for *Glrx* shRNA and mVenus, a variant of the yellow fluorescent protein, using the purification protocol without discontinuous iodixanol gradient.

We have previously reported that *Glrx*-deficient mice develop obesity and non-alcoholic fatty liver (NAFL) disease⁵⁰. On the other hand, *Glrx* deficiency promotes angiogenesis in ischemic limbs in this mouse strain⁵¹. *Glrx* is a thiol transferase which removes GSH adducts from proteins⁵². GSH adducts are generated through oxidative post-translational modifications, especially at cysteine residues⁵³, and regulate the function of transcription factors^{51,54}, cytoskeletal assembly⁵⁵, and signaling molecules^{56,57}. Since the role of *Glrx* differs between tissues, there is the need to locally inhibit *Glrx* expression or manipulate *Glrx* expression in a tissue-specific manner.

AAV2-DJ has a hybrid capsid generated by DNA shuffling from different native serotypes¹⁰. These AAV vectors are considered to have high infectivity to tissues and cells compared to other native serotypes.

Primary mouse hepatocytes in culture transduced with AAV2-DJ-sh*Glrx*-mVenus exhibited a \sim 70% knock-down of *Glrx* expression compared to AAV2-DJ-shControl-mVenus infected cells (Fig. 4A). Quiescent confluent C2C12 cells showed similar results for mRNA expression and protein levels after 4 days (Fig. 4B,C). AAV2-DJ/8 was unable to transduce cultured cells (data not shown). AAV-delivered shRNA is much more potent compared to the application of siRNA, with which we have experienced difficulties in silencing *Glrx* gene expression in differentiated C2C12 cells.

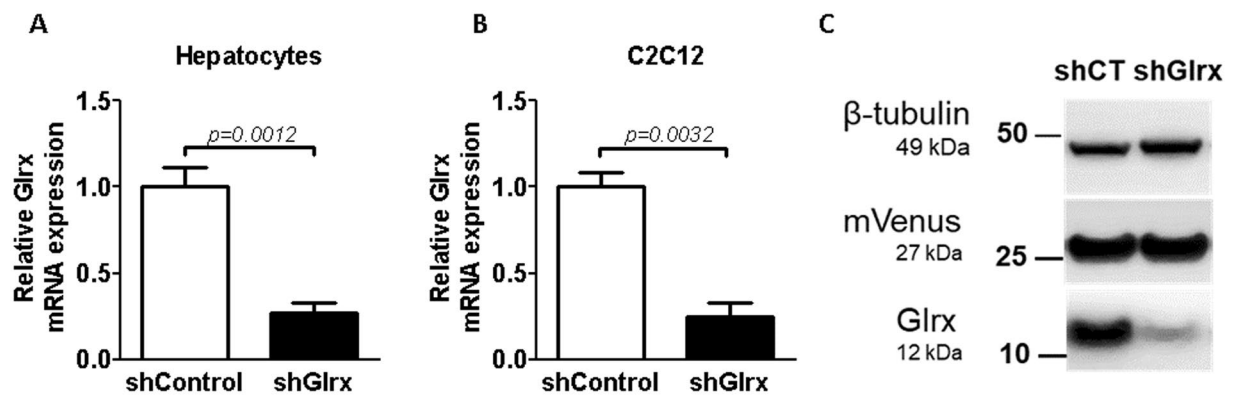


Figure 4. mRNA and protein levels in primary hepatocytes and C2C12 cells infected with AAV2-DJ-shGlx-Venus. Glrx mRNA levels in primary hepatocytes (A), and C2C12 cells (B) after 6 and 4 days post infection, respectively, with either AAV2-DJ-shControl-mVenus (shControl) or AAV2-DJ-shGlx-mVenus (shGlx). Glrx mRNA expression was normalized to Actb mRNA, and the fold-change was compared to shControl (n = 6–7; SD). (C) Glrx and Venus protein levels in C2C12 cells from (B). β -tubulin served as a loading control. shCT: C2C12 cells infected with AAV2-DJ-shControl-mVenus.

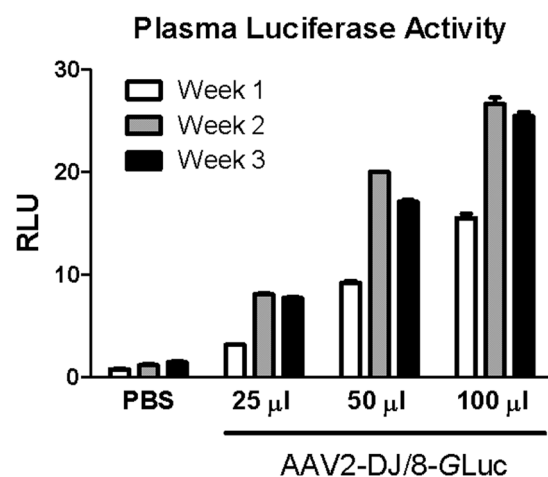


Figure 5. Relative plasma luciferase activity. Relative plasma luciferase activity of AAV2-DJ/8-GLuc (1.5×10^{11} vg/ μ l) tail vein injected male mice compared to PBS injected controls. Blood was collected from the tail vein at 1, 2, and 3 weeks after injection, and luciferase activity was measured. n = 4 per condition, SEM.

Testing AAVs *in vivo*. Surprisingly, our first *in vivo* experiment with retro-orbitally injected AAV2-DJ/8-shGlx-mVenus following our purification protocol without discontinuous iodixanol gradient had little effect in mouse liver (data are not shown). We suspected impurities in the AAV preparations caused low-grade inflammation, which compromised virus infectivity and knockdown of Glrx in the liver, an effect also observed by others³⁸. Thus, to quickly evaluate the onset and stability of gene expression, we generated an AAV expressing secreted *Gaussia* luciferase (AAV2-DJ/8-GLuc) and further purified the virus via a discontinuous iodixanol gradient, which resulted in a very pure AAV (>90%) as measured by silver staining. We injected the virus via the tail vein, and measured luciferase activity in tail vein bleeds. Groups of four male mice received either PBS or three different doses of AAV2-DJ/8-GLuc. Luciferase activity stabilized between week one and two and maintained comparable levels for at least three weeks. Also, luciferase activity increased dose-dependently (Fig. 5).

Subsequent purification of AAV2-DJ/8-shGlx-mVenus via a discontinuous iodixanol gradient resulted in a 66% knockdown of Glrx mRNA in the liver compared to mice injected with AAV2-DJ/8-shControl-mVenus (Fig. 6A). Hepatic Glrx protein expression almost disappeared in AAV2-DJ/8-shGlx-mVenus administered mice but remained unaffected in AAV2-DJ/8-shControl-mVenus injected mice (Fig. 6B).

We detected viral infection of the liver by immunohistology using a GFP-antibody that cross-reacts with mVenus, the yellow fluorescent protein variant co-expressed by AAV2-DJ/8-shGlx-mVenus. Because retro-orbitally injected AAV2-DJ/8-shGlx-mVenus entered the liver via the hepatic artery (Fig. 6C, top row), mVenus expression was highest around the triad (hepatic artery, bile duct, and portal vein; T). Viral particles decreased while traveling to the central vein, which explains the gradual decrease (white arrow) of mVenus expression towards the central vein (C), an effect referred to as zonation of the liver acinus. Liver sections of AAV2-DJ/8-shGlx-mVenus injected mice stained with secondary antibody only (middle row), or saline-injected mice (top row) showed no mVenus expression.

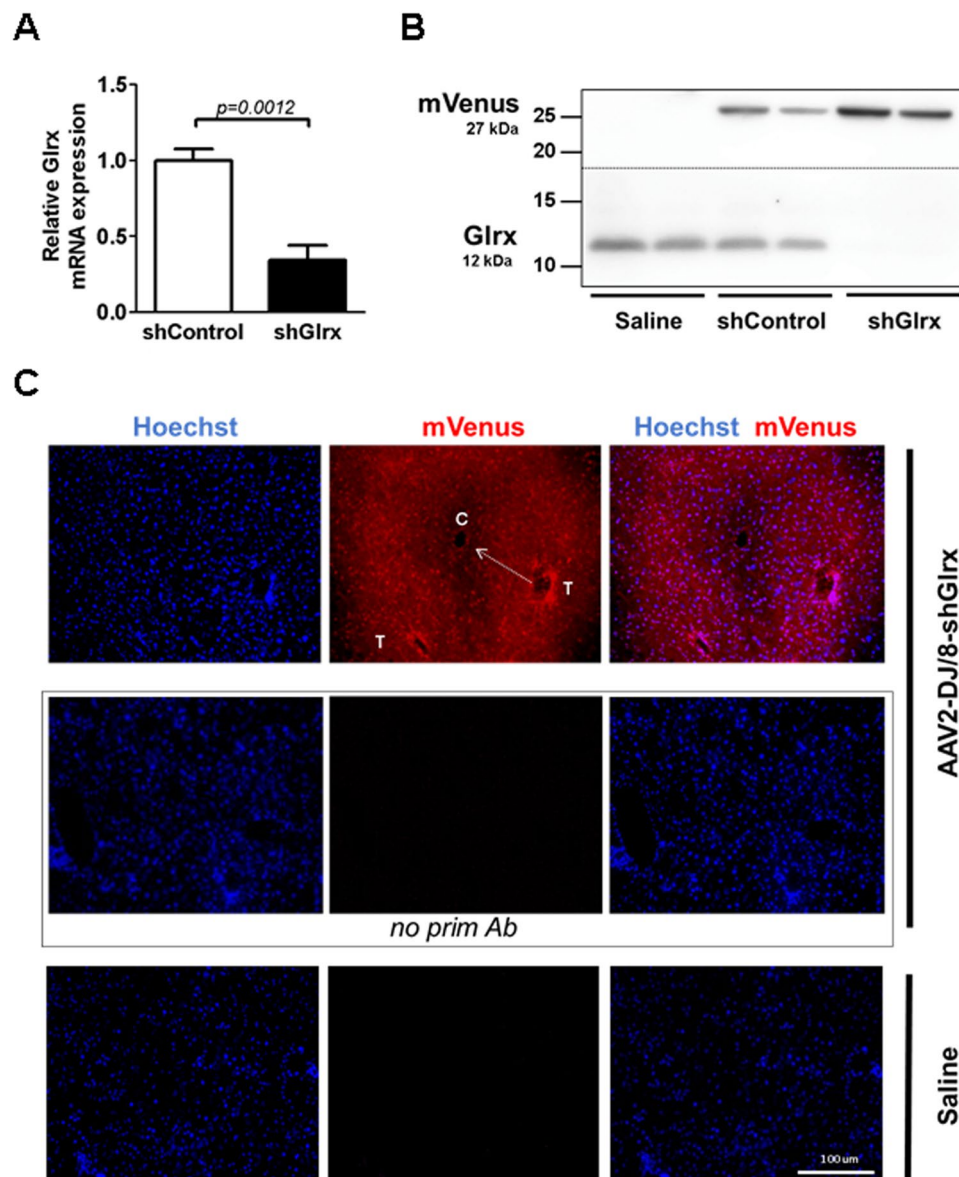


Figure 6. mRNA and protein expression of Glrx in mouse liver. (A) Glrx mRNA expression levels in livers of C57BL/6J mice two weeks after administration of AAV2-DJ/8-shControl-mVenus (shControl) or AAV2-DJ/8-shGlrX-mVenus (shGlrX). Gene expression was measured by RT-qPCR and the statistical analysis was performed using the two-tailed Mann-Whitney test. Statistical differences ($n = 6-7$; $P < 0.05$; SD) were compared to shControl. (B) Western blot analysis of the liver samples described in (A). The membrane (dotted line indicates the cut) was probed for mVenus and Glrx expression 2 weeks post AAV injection. (C) Liver sections from an AAV2-DJ/8-shGlrX-mVenus injected mouse showed a strong fluorescence signal of mVenus (top row, red color) in cytoplasm and nuclei. Nuclei were counterstained with Hoechst 33342. The mVenus signal was most intense around the triad (T) and faded towards (arrow) the central vein (C), showing zonation across the liver acinus. Neither liver sections of AAV2-DJ/8-shGlrX-mVenus injected mice, incubated with secondary antibody alone (middle row), nor saline-injected mice exhibited a significant mVenus signal at identical exposure time settings. Scale bar denotes 100 μm .

Testing AAVs in mouse skeletal muscle. AAV injection into the skeletal muscle was more challenging than previously anticipated. Similar to the liver, the virus requires high purity and a high viral titer for injection of small volumes into the muscle. We examined the tissue-specific expression of AAV2-6-shGlrX-mVenus since this capsid has a better tissue tropism for skeletal muscle⁵⁹⁻⁶². Also, using a different capsid further supports the general applicability of our protocol. After *IM* injection, we detected a high level of mVenus expression after 3 weeks in the injected gastrocnemius muscle (Fig. 7A, left) but not in the non-injected muscle, heart, or liver (Fig. 7C). These data demonstrate *IM* injection of AAV2-6 restricts the infection to the muscle.

Although AAV2-6 efficiently transduced mVenus expression in skeletal muscle and AAV2-DJ-shGlrX-mVenus suppressed Glrx expression in C2C12 cells (Fig. 4B,C), *in vivo* inhibition of muscle Glrx by AAV2-6-shGlrX-m

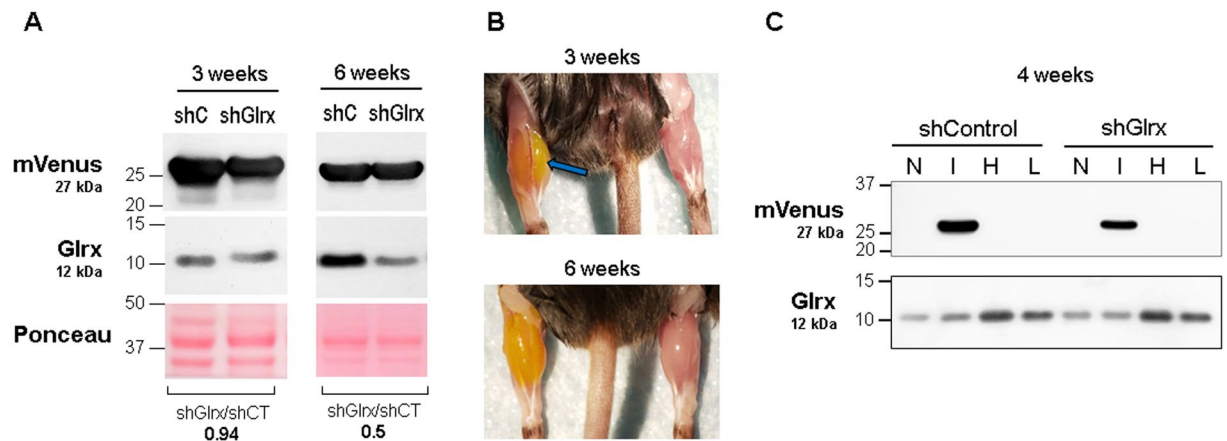


Figure 7. AAV2-6 mVenus transduced skeletal muscle. AAV2-6-shGlx-mVenus *IM* injection induced in mVenus protein expression after 2 weeks but inhibition of Glrx expression occurred only after 6 weeks. **(A)** mVenus and Glrx expression in AAV-injected muscles. Mice were euthanized at 3 and 6 weeks after *IM* injection. shCT: AAV expressing short hairpin control. shGlx: AAV expressing short hairpin RNA to Glrx. At 6 weeks, shGlx inhibited Glrx expression to half of the control. Ponceau staining is shown as protein loading control. **(B)** *Upper panel:* The AAV-injected muscle turned yellow by mVenus expression and was swollen (arrow) compared to the non-injected muscle at 3 weeks. *Lower panel:* After 6 weeks, the muscle size appeared similar to the non-injected muscle. **(C)** mVenus and Glrx expression in other organs at 4 weeks after AAV *IM* injection. mVenus only expressed in the injected gastrocnemius muscle (I), but the AAV did not leak into the non-injected muscle (N), heart (H), or liver (L). AAV-shGlx-injected muscles did not decrease Glrx protein expression at 4 weeks post-injection.

Venus proved challenging. After 3–4 weeks of AAV2-6-shGlx-mVenus *IM* injection, the protein level of Glrx in the muscle remained unchanged compared to control-AAV injected or non-injected muscle (Fig. 7A, left). The purity of AAVs was similar to that of AAV2-DJ/8-shGlx-mVenus, which inhibited liver Glrx expression after 2 weeks. However, *IM* injection may cause local stress and inflammation of the muscle compared to intravenous injection. The muscle expressed mVenus highly and appeared yellowish and swollen after 3 weeks (Fig. 7B). After 6 weeks of AAV2-6-shGlx-mVenus *IM* injection, the muscle inflammation resolved, and Glrx expression decreased in the AAV2-6-shGlx-mVenus injected muscle compared to the AAV2-6-shControl-mVenus injected muscle (Fig. 7A,B).

Discussion

We established an improved protocol that allows fast and efficient purification of AAVs independent of the serotype. Our protocol is composed of purifications from both HEK293T cell lysates and culture medium. Optimization of the culture medium demonstrated that excess glucose adversely affects viral production by promoting acidification, presumably through excessive glycolysis. As established for other cell types and viruses glutaminolysis is more critical to sustaining cell metabolism and robust virus production^{31–35}. Glutamine feeds directly into the citric acid cycle to provide energy but also contributes to anaplerosis, a process to replenish the cycle with metabolites used in anabolic reactions such as amino acid synthesis. Therefore, we recommend the use of pH stabilized low glucose DMEM supplemented with stable glutamine (GlutaMAX).

Furthermore, the AAV samples with discontinuous iodixanol gradient purification improved the purity of AAVs. Using an AAV2-DJ/8-shGlx-mVenus but omitting the iodixanol purification could not silence the expression of hepatic Glrx *in vivo*, suggesting contaminants cause inflammation and induce endogenous protein, whereas the same AAV after iodixanol purification efficiently attenuated the gene expression (data not shown). The results indicate the iodixanol purification as a necessary step to obtain AAVs that are suitable for *in vivo* use. Zolotukhin *et al.* also showed that purification with iodixanol was useful to obtain viruses of higher titer and purity compared to the cesium chloride ultracentrifugation method²³. Because of minimal ionic and osmotic effects of iodixanol, gradient fractions after the final purification can be directly used without dialysis in cell and animal experiments. However, iodixanol in high amounts may lead to renal dysfunction. In our study, we obtained AAVs with a purity of greater than 90% in high yields of 10^{10} – 10^{11} vg/μl. Also, our method needs only seven days from transfection with the AAV plasmids until the final viral suspension for *in vivo* use. Using primers against the ITRs sequences for AAV titer determinations with qPCR may overestimate the viral particle content caused by the amplification of contaminating incomplete viral particles. The sequence coding for shRNAs may form stable DNA structures that mimic ITRs leading to early termination of viral single-stranded DNA (ssDNA) replication and generation of incomplete AAVs⁶³. We applied a different shRNA sequence design, introduced by Miyagishi *et al.*, to minimize the production of incomplete particles¹⁹. As our experiments in cultured cells and *in vivo* demonstrated, we obtained sufficient viral particles to suppress Glrx gene expression.

AAVs have been used to express transgenes *in vivo*, but *in vitro* applications are rare. However, as we show here using primary mouse hepatocytes and skeletal muscle-derived C2C12 cells, AAV2-DJ efficiently infects cells

in vitro. The AAV2-DJ vector is a chimeric virus with a hybrid capsid from different wild-type AAVs, and predominantly shows high homology to wild-type AAV-2, AAV2-8, and AAV2-9, the three most efficient serotypes for mouse liver infection^{10,64}. AAV2-DJ performs more effectively in various types of cells compared to the other eight primary AAV serotypes¹⁰ and is highly potent in mouse liver⁶⁴. The variant AAV2-DJ/8 lacks a heparin-binding domain, which attenuates its efficiency *in vitro*, but broadens tissue distribution *in vivo*¹⁰ and can penetrate the central nervous system.

Different AAV serotypes control tissue tropism to a certain degree. Systemic administration of AAV2-DJ or AAV2-DJ/8 shows a favorable expression in liver^{10,64}. Gene delivery applications to the muscle of dystrophic mice widely use the AAV2-6 vector, but the vascular delivery of AAV2-6 transduces both cardiac and skeletal muscles^{59,60}. We demonstrated that *IM* injection of AAV2-6-shGlx-mVenus resulted in mVenus expression in the muscle but not in the heart or liver, suggesting *IM*-injected AAV2-6 may transduce more selectively the skeletal muscle. The use of tissue-specific promoters in AAV-mediated gene expression system, such as albumin (Alb) and thyroxine-binding globulin (TBG), can improve targeted AAV-mediated gene expression⁵. Exchanging promoters to target a specific tissue or cell type is desirable for AAV-mediated gene therapy.

Since systemically administered AAVs may affect other organs, we performed *IM* injection to restrict the AAV-mediated gene suppression of Glrx to the skeletal muscle. AAVs are widely used for gene delivery to the muscle^{58,65}, and intramuscular injection can be successfully delivered and stably expressed over five months in the mouse muscle⁶⁶. We detected mVenus expression in the muscle already after 3 weeks. However, suppression of muscle Glrx expression by AAV2-6-shGlx took longer, and we detected it decreased after 6 weeks. This long delay was unexpected because the systemically injected AAV2-DJ/8-shGlx-mVenus markedly suppressed liver Glrx expression after 2 weeks. We speculate that Glrx protein turnover in the muscle may be slower than in the liver.

Furthermore, the injected muscle looked yellowish and swollen, and the AAV may induce inflammatory genes in the muscle at 3 weeks. The injected AAV2-6-shGlx-mVenus also expresses mVenus as a marker. It is important to remark that fluorescent proteins such as GFP, and variants thereof, may produce superoxide and cause oxidative stress⁶⁷. Notably, for therapeutic purposes of minimizing inflammation and off-target effects, we believe that mVenus should be omitted. Glrx is known as a NF- κ B responsive gene⁶⁸. We speculate that AAV-induced inflammatory responses in the muscle may activate the NF- κ B pathway and upregulate Glrx expression⁶⁸, counteracting the inhibition by shGlx. Clerk *et al.* also observed inflammatory cell infiltration into the injected muscle up to one month after *IM* AAV injection⁶⁶. Even though AAVs are supposed to cause less inflammation compared to adenovirus, one should take into account inflammatory responses caused by AAV injection. Also, intravascular injection of AAVs causes an immune response to the AAV capsid and inflammation in muscles, which is improved by a short course of an immunosuppressant⁶⁰. Clinically, naturally-occurring neutralizing antibodies to AAV capsids can attenuate AAV-mediated gene therapy. Interestingly, in the presence of a neutralizing antibody to AAV2-8 capsid, *IM* injection of AAV2-8 still delivers the transgene to muscles, but abolishes gene expression in liver⁶⁹, suggesting the usefulness of *IM* injection to induce transgene expression in muscles of people with naturally-occurring antibodies to AAVs.

In summary, we presented a refined, rapid, and economical protocol to produce and purify AAVs, which efficiently transduce genes *in vitro* and *in vivo*. Iodixanol purification is helpful to eliminate contaminants and thus improve AAV purity, diminish inflammation, and improve viral transduction *in vivo*.

References

- Kotterman, M. A. & Schaffer, D. V. Engineering adeno-associated viruses for clinical gene therapy. *Nat. Rev. Genet.* **15**, 445–451 (2014).
- Rangarajan, S. *et al.* AAV5–Factor VIII Gene Transfer in Severe Hemophilia A. *N. Engl. J. Med.* **377**, 2519–2530 (2017).
- Kaplitt, M. G. *et al.* Safety and tolerability of gene therapy with an adeno-associated virus (AAV) borne GAD gene for Parkinson's disease: an open label, phase I trial. *Lancet (London, England)* **369**, 2097–105 (2007).
- Bainbridge, J. W. B. *et al.* Effect of Gene Therapy on Visual Function in Leber's Congenital Amaurosis. *N. Engl. J. Med.* **358**, 2231–2239 (2008).
- Kattenhorn, L. M. *et al.* Adeno-Associated Virus Gene Therapy for Liver Disease. *Hum. Gene Ther.* **27**, 947–961 (2016).
- Kotin, R. M., Linden, R. M. & Berns, K. I. Characterization of a preferred site on human chromosome 19q for integration of adeno-associated virus DNA by non-homologous recombination. *EMBO J.* **11**, 5071–8 (1992).
- Duan, D. *et al.* Circular intermediates of recombinant adeno-associated virus have defined structural characteristics responsible for long-term episomal persistence in muscle tissue. *J. Virol.* **72**, 8568–77 (1998).
- Kaplitt, M. G. *et al.* Long-term gene transfer in porcine myocardium after coronary infusion of an adeno-associated virus vector. *Ann. Thorac. Surg.* **62**, 1669–76 (1996).
- Grimm, D. & Kleinschmidt, J. A. Progress in Adeno-Associated Virus Type 2 Vector Production: Promises and Prospects for Clinical Use. *Hum. Gene Ther.* **10**, 2445–2450 (1999).
- Grimm, D. *et al.* *In vitro* and *in vivo* gene therapy vector evolution via multispecies interbreeding and retargeting of adeno-associated viruses. *J. Virol.* **82**, 5887–911 (2008).
- Addgene. AAV Production in HEK293 Cells. Available at, <https://www.addgene.org/protocols/aav-production-hek293-cells/>, (Accessed: 22nd August 2018) (2018).
- Vandenbergh, L. H. *et al.* Efficient serotype-dependent release of functional vector into the culture medium during adeno-associated virus manufacturing. *Hum. Gene Ther.* **21**, 1251–7 (2010).
- Piras, B. A. *et al.* Distribution of AAV8 particles in cell lysates and culture media changes with time and is dependent on the recombinant vector. *Mol. Ther. - Methods Clin. Dev.* **3**, 16015 (2016).
- Lock, M. *et al.* Rapid, simple, and versatile manufacturing of recombinant adeno-associated viral vectors at scale. *Hum. Gene Ther.* **21**, 1259–71 (2010).
- Okada, T. *et al.* Scalable Purification of Adeno-associated Virus Serotype 1 (AAV1) and AAV8 Vectors, Using Dual Ion-Exchange Adsorptive Membranes. *Hum. Gene Ther.* **20**, 1013–1021 (2009).
- Benskey, M. J., Sandoval, I. M. & Manfredsson, F. P. Continuous Collection of Adeno-Associated Virus from Producer Cell Medium Significantly Increases Total Viral Yield. *Hum. Gene Ther. Methods* **27**, 32–45 (2016).
- Hou, X. *et al.* SIRT1 regulates hepatocyte lipid metabolism through activating AMP-activated protein kinase. *J Biol Chem* **283**, 20015–26 (2008).

18. Xia, X. G. *et al.* An enhanced U6 promoter for synthesis of short hairpin RNA. *Nucleic Acids Res.* **31**, e100 (2003).
19. Makoto Miyagishi, Hidetoshi Sumimoto, Hiroyuki Miyoshi, Yutaka Kawakami, Kazunari Taira. Optimization of an siRNA-expression system with an improved hairpin and its significant suppressive effects in mammalian cells. *The Journal of Gene Medicine* **6**(7), 715–723 (2004).
20. Fukumoto, Y. *et al.* Cost-effective gene transfection by DNA compaction at pH 4.0 using acidified, long shelf-life polyethylenimine. *Cytotechnology* **62**, 73–82 (2010).
21. Guo, P. *et al.* A simplified purification method for AAV variant by polyethylene glycol aqueous two-phase partitioning. *Bioengineered* **4**, 103–106 (2013).
22. Guo, P. *et al.* Rapid and simplified purification of recombinant adeno-associated virus. *J. Virol. Methods* **183**, 139–146 (2012).
23. Zolotukhin, S. *et al.* Recombinant adeno-associated virus purification using novel methods improves infectious titer and yield. *Gene Ther.* **6**, 973–85 (1999).
24. Hermens, W. T. *et al.* Purification of recombinant adeno-associated virus by iodixanol gradient ultracentrifugation allows rapid and reproducible preparation of vector stocks for gene transfer in the nervous system. *Hum. Gene Ther.* **10**, 1885–91 (1999).
25. Aurnhammer, C. *et al.* Universal Real-Time PCR for the Detection and Quantification of Adeno-Associated Virus Serotype 2-Derived Inverted Terminal Repeat Sequences. *Hum. Gene Ther. Methods* **23**, 18–28 (2012).
26. Kohlbrenner, E. *et al.* Quantification of AAV particle titers by infrared fluorescence scanning of coomassie-stained sodium dodecyl sulfate-polyacrylamide gels. *Hum. Gene Ther. Methods* **23**, 198–203 (2012).
27. Johnson, F. B., Ozer, H. L. & Hoggan, M. D. Structural proteins of adenovirus-associated virus type 3. *J. Virol.* **8**, 860–63 (1971).
28. Becerra, S. P., Koczot, F., Fabisch, P. & Rose, J. A. Synthesis of adeno-associated virus structural proteins requires both alternative mRNA splicing and alternative initiations from a single transcript. *J. Virol.* **62**, 2745–54 (1988).
29. Atkinson, E. M., Takeya, R. K. & Aranha, I. L. Methods for generating high titer helper-free preparations of released recombinant AAV vectors (2003).
30. Imamoto, Y., Tanaka, H., Takahashi, K., Konno, Y. & Suzawa, T. Advantages of AlaGln as an additive to cell culture medium: use with anti-CD20 chimeric antibody-producing POTEILLIGENT™ CHO cell lines. *Cytotechnology* **65**, 135–143 (2013).
31. Fontaine, K. A., Camarda, R. & Lagunoff, M. Vaccinia Virus Requires Glutamine but Not Glucose for Efficient Replication. *J. Virol.* **88**, 4366–4374 (2014).
32. Hosios, A. M. *et al.* Amino Acids Rather than Glucose Account for the Majority of Cell Mass in Proliferating Mammalian Cells. *Dev. Cell* **36**, 540–9 (2016).
33. Reitzer, L. J., Wice, B. M. & Kennell, D. Evidence that glutamine, not sugar, is the major energy source for cultured HeLa cells. *J. Biol. Chem.* **254**, 2669–76 (1979).
34. Spolarics, Z., Lang, C. H., Bagby, G. J. & Spitzer, J. J. Glutamine and fatty acid oxidation are the main sources of energy for Kupffer and endothelial cells. *Am. J. Physiol.* **261**, G185–90 (1991).
35. Tohyama, S. *et al.* Glutamine Oxidation Is Indispensable for Survival of Human Pluripotent Stem Cells. *Cell Metab.* **23**, 663–674 (2016).
36. Arden, E. & Metzger, J. M. Inexpensive, serotype-independent protocol for native and bioengineered recombinant adeno-associated virus purification. *J. Biol. methods* **3**, 38 (2016).
37. Grieger, J. C., Choi, V. W. & Samulski, R. J. Production and characterization of adeno-associated viral vectors. *Nat. Protoc.* **1**, 1412–28 (2006).
38. Sakamoto, S. *et al.* Method for manufacturing non-enveloped virus (2016).
39. Salganik, M. *et al.* Evidence for pH-dependent protease activity in the adeno-associated virus capsid. *J. Virol.* **86**, 11877–85 (2012).
40. François, A. *et al.* Accurate Titration of Infectious AAV Particles Requires Measurement of Biologically Active Vector Genomes and Suitable Controls. *Mol. Ther. Methods Clin. Dev.* **10**, 223–236 (2018).
41. Fagone, P. *et al.* Systemic errors in quantitative polymerase chain reaction titration of self-complementary adeno-associated viral vectors and improved alternative methods. *Hum. Gene Ther. Methods* **23**, 1–7 (2012).
42. Werling, N. J., Satkunanathan, S. & Thorpe, R. & Zhao, Y. Systematic Comparison and Validation of Quantitative Real-Time PCR Methods for the Quantitation of Adeno-Associated Viral Products. *Hum. Gene Ther. Methods* **26**, 82–92 (2015).
43. D'Costa, S. *et al.* Practical utilization of recombinant AAV vector reference standards: focus on vector genomes titration by free ITR qPCR. *Mol. Ther. Methods Clin. Dev.* **5**, 16019 (2016).
44. Hauck, B. *et al.* Undetectable Transcription of cap in a Clinical AAV Vector: Implications for Preformed Capsid in Immune Responses. *Mol. Ther.* **17**, 144–152 (2009).
45. Wright, J. F. Transient Transfection Methods for Clinical Adeno-Associated Viral Vector Production. *Hum. Gene Ther.* **20**, 698–706 (2009).
46. Potter, M., Chesnut, K., Muzyczka, N., Flotte, T. & Zolotukhin, S. Streamlined large-scale production of recombinant adeno-associated virus (rAAV) vectors. *Methods Enzymol.* **346**, 413–30 (2002).
47. Andreucci, M., Faga, T., Serra, R., De Sarro, G. & Michael, A. Update on the renal toxicity of iodinated contrast drugs used in clinical medicine. *Drug. Healthc. Patient Saf.* **9**, 25–37 (2017).
48. Yao, L. *et al.* Evaluation of urine fibrinogen level in a murine model of contrast-induced nephropathy. *Vascular* **24**, 273–278 (2016).
49. Klöw, N. E. *et al.* Iodixanol in cardioangiography in patients with coronary artery disease. Tolerability, cardiac and renal effects. *Acta Radiol.* **34**, 72–7 (1993).
50. Shao, D. *et al.* Glutaredoxin-1 Deficiency Causes Fatty Liver and Dyslipidemia by Inhibiting Sirtuin-1. *Antioxidants Redox Signal.* **27** (2017).
51. Watanabe, Y. *et al.* Glutathione adducts induced by ischemia and deletion of glutaredoxin-1 stabilize HIF-1 α and improve limb revascularization. *Proc. Natl. Acad. Sci. USA* **113**, 6011–6 (2016).
52. Matsui, R., Watanabe, Y. & Murdoch, C. E. Redox regulation of ischemic limb neovascularization - What we have learned from animal studies. *Redox Biol.* **12**, 1011–1019 (2017).
53. Chung, H. S., Wang, S.-B., Venkatraman, V., Murray, C. I. & Van Eyk, J. E. Cysteine oxidative posttranslational modifications: emerging regulation in the cardiovascular system. *Circ. Res.* **112**, 382–92 (2013).
54. Shelton, M. D., Kern, T. S. & Mieyal, J. J. Glutaredoxin regulates nuclear factor kappa-B and intercellular adhesion molecule in Müller cells: model of diabetic retinopathy. *J. Biol. Chem.* **282**, 12467–74 (2007).
55. Wang, J. *et al.* Stable and controllable RNA interference: Investigating the physiological function of glutathionylated actin. *Proc. Natl. Acad. Sci. USA* **100**, 5103–6 (2003).
56. Mieyal, J. J., Gallogly, M. M., Qanungo, S., Sabens, E. A. & Shelton, M. D. Molecular mechanisms and clinical implications of reversible protein S-glutathionylation. *Antioxid. Redox Signal.* **10**, 1941–88 (2008).
57. Pimentel, D. *et al.* Regulation of cell physiology and pathology by protein S-glutathionylation: lessons learned from the cardiovascular system. *Antioxid. Redox Signal.* **16**, 524–42 (2012).
58. Ayuso, E. *et al.* High AAV vector purity results in serotype- and tissue-independent enhancement of transduction efficiency. *Gene Ther.* **17**, 503–10 (2010).
59. Gregorevic, P. *et al.* rAAV6-microdystrophin preserves muscle function and extends lifespan in severely dystrophic mice. *Nat. Med.* **12**, 787–9 (2006).
60. Gregorevic, P. *et al.* Evaluation of vascular delivery methodologies to enhance rAAV6-mediated gene transfer to canine striated musculature. *Mol. Ther.* **17**, 1427–33 (2009).

61. Bulaklak, K. & Xiao, X. Therapeutic advances in musculoskeletal AAV targeting approaches. *Curr. Opin. Pharmacol.* **34**, 56–63 (2017).
62. Marshall, J. P. S. *et al.* Skeletal muscle-specific overexpression of heat shock protein 72 improves skeletal muscle insulin-stimulated glucose uptake but does not alter whole body metabolism. *Diabetes, Obes. Metab.* **20**, 1928–1936 (2018).
63. Xie, J. *et al.* Short DNA Hairpins Compromise Recombinant Adeno-Associated Virus Genome Homogeneity. *Mol. Ther.* **25**, 1363–1374 (2017).
64. Liu, J. & Moon, Y.-A. Simple Purification of Adeno-Associated Virus-DJ for Liver-Specific Gene Expression. *Yonsei Med. J.* **57**, 790–4 (2016).
65. Boisgerault, F. & Mingozzi, F. The Skeletal Muscle Environment and Its Role in Immunity and Tolerance to AAV Vector-Mediated Gene Transfer. *Curr. Gene Ther.* **15**, 381–94 (2015).
66. Clark, K. R., Sferra, T. J. & Johnson, P. R. Recombinant Adeno-Associated Viral Vectors Mediate Long-Term Transgene Expression in Muscle. *Hum. Gene Ther.* **8**, 659–669 (1997).
67. Ganini, D. *et al.* Fluorescent proteins such as eGFP lead to catalytic oxidative stress in cells. *Redox Biol.* **12**, 462–468 (2017).
68. Aesif, S. W. *et al.* Activation of the glutaredoxin-1 gene by nuclear factor κ B enhances signaling. *Free Radic. Biol. Med.* **51**, 1249–1257 (2011).
69. Greig, J. A. *et al.* Intramuscular administration of AAV overcomes pre-existing neutralizing antibodies in rhesus macaques. *Vaccine* **34**, 6323–6329 (2016).

Acknowledgements

This work was supported by NIH grants R01 DK103750, R01 HL133013, and R03 AG 051857, American Heart Association “Grant in Aid” 16GRNT27660006, European Cooperation in Science and Technology (COST Action BM1203/EU-ROS), and the Metabolic Clinical Research Collaborative. This work was also supported by the NIH/Boston University CTSI grant 1UL1TR001430 to M.M.B., and R.M.. M.M.B. was also supported by the Evans Junior Faculty Research Award by the Department of Medicine of Boston University. B.F. and A.F. were supported by NIH T32 HL07224 Multidisciplinary Training in Cardiovascular Research through the Whitaker Cardiovascular Institute. T.K. was supported by the National Defense Medical College foreign exchange program. T.K., Y.I., and T.A. were supported by a grant awarded by the Japanese Ministry of Defense, and MEXT/JSPS KAKENHI Grant-in-Aid for Scientific Research (JP 18H02815 and JP 18K8120). The grant from Kilo Diabetes & Vascular Research Foundation supported Y.I. for development of plasmid works. I.L. was supported by the American Heart Association 15FTF25890062 fellowship. The article contents are solely the responsibility of the authors and do not necessarily represent the official views of the awarding offices. We thank Drs M. Kirber, F. Seta, and L. Deng and the Boston University School of Medicine “Analytical Instrumentation,” “Cellular Imaging,” and “Metabolic Phenotyping” cores for their technical support. We acknowledge the contributions of our RISE students Diane Da-Hyun Lee, Prashant Malayala, Ellie Cheong, and Leslie Pu and UROP student Jeffrey Leong to this study as well as the RISE and UROP programs for financial support. We appreciate the help of Dominique Croteau for proofreading and revising our manuscript.

Author Contributions

T.K. and B.F. produced the virus, performed animal experiments, and revised the manuscript. S.D. prepared and tested viral plasmids. Y.T. and Q.S. conducted and reviewed the immunohistology. A.F. optimized the AAV production cell culture medium. I.L. and T.A. provided critical suggestions regarding data analysis and manuscript revision. Y.I. and D.R.P. established AAV production, cloned plasmids, and offered critical suggestions regarding the manuscript. R.M. and M.M.B. designed the research, interpreted the data, and wrote the paper.

Additional Information

Supplementary information accompanies this paper at <https://doi.org/10.1038/s41598-019-49624-w>.

Competing Interests: The authors declare no competing interests.

Publisher’s note Springer Nature remains neutral with regard to jurisdictional claims in published maps and institutional affiliations.



Open Access This article is licensed under a Creative Commons Attribution 4.0 International License, which permits use, sharing, adaptation, distribution and reproduction in any medium or format, as long as you give appropriate credit to the original author(s) and the source, provide a link to the Creative Commons license, and indicate if changes were made. The images or other third party material in this article are included in the article’s Creative Commons license, unless indicated otherwise in a credit line to the material. If material is not included in the article’s Creative Commons license and your intended use is not permitted by statutory regulation or exceeds the permitted use, you will need to obtain permission directly from the copyright holder. To view a copy of this license, visit <http://creativecommons.org/licenses/by/4.0/>.

© The Author(s) 2019